Title: The level of occlusion of included bark affects the strength of bifurcations in hazel (*Corylus avellana* L.)

Authors: **Duncan Slater**, senior lecturer in arboriculture, Myerscough College, St. Michaels Road, Bilsborrow, PRESTON PR3 0RY
Telephone: 01995 642222 ext. 2304 Fax: 01995 642333
Email: dslater@myerscough.ac.uk

Prof. Roland Ennos, School of Biological, Biomedical and Environmental Sciences, University of Hull, Cottingham Road, Kingston-upon-Hull HU6 7RX
Email: R.Ennos@hull.ac.uk

Manuscript reference: AUF-14-0031

Date of first submission: 09.05.2014
Date of resubmission: 03.10.2014
Date of submission of revised version: 12.01.2015

Number of tables: 1
Number of figures: 11

Word count: 6815

Abstract

Bark-included junctions in trees are considered a defect as the bark weakens the union between the branches. To more accurately assess this weakening effect, 241 bifurcations from young specimens of *hazel (Corylus avellana* L.), of which 106 had bark inclusions, were harvested and subjected to rupture tests. Three-point bending of the smaller branches acted as a benchmark for the relative strength of the bifurcations.

Bifurcations with included bark failed at higher displacements and their modulus of rupture was 24% lower than normally-formed bifurcations, while stepwise regression showed that the best predictors of strength in these bark-included bifurcations were the diameter ratio and width of the bark inclusion, which explained 16.6% and 8.1% of the variability respectively. Cup-shaped bark-included bifurcations where included bark was partially occluded by xylem were found to be on average 36% stronger than those where included bark was situated at the bifurcation apex.

These findings show that there are significant gradations in the strength of bark-included bifurcations in juvenile hazel trees that relate directly to the level of occlusion of the bark into the bifurcation. It therefore may be possible to assess the extent of the defect that a bark-included bifurcation represents in a tree by assessing the relative level of occlusion of the included bark.

Keywords: bifurcation; *Corylus avellana*; hazel; included bark; rupture tests; three-point bending

Introduction

Junctions in trees that are separated by bark being included in their union are frequently found in urban and forest trees (Lonsdale, 1999). Such junctions have a reputation of being structural flaws in tree crowns (Shigo, 1989; Lonsdale, 2000; Harris, Clark and Matheny, 2004; Gilman, 2011), and they are commonly recorded as a defect by tree assessors and others with responsibility for the safety of people and property adjacent to trees (Matheny and Clark, 1994; Mattheck and Breloer, 1994).

Where only two branches arise from a junction in a tree, this is formally referred to as a bifurcation. It has been established that the 'diameter ratio' between the two branches that arise from a bifurcation in a tree has a substantial effect on its mechanical strength and failure mode (Gilman, 2003). The 'diameter ratio' is defined as the ratio between the basal diameters of the smaller and larger branch, measured just above the point of their attachment to each other at the bifurcation, and is often also referred to as the 'aspect ratio' (Gilman, 2003). Kane *et al.* (2008) found through rupture testing that bifurcations formed in young trees of three species (*Acer rubrum* L., *Quercus acutissima* Carruthers and *Pyrus calleryana* Decne.) that had a diameter ratio of 70% or higher were only half as strong as those that had a clearly subsidiary branch. Additionally, these researchers found that the fracture surfaces of bifurcations with a low diameter ratio showed that xylem tissues of the smaller branch were embedded within the larger branch; in contrast, co-dominant stems exhibited relatively flat fracture surfaces with little to no embedding of tissues.

Two distinct failure modes occur in higher diameter ratio bifurcations of hazel (*Corylus avellana* L.) when they are subjected to tensile loading, and these have been defined by Slater and Ennos (2013) as Type I and Type II failure modes. In the Type I failure mode, which tends to occur at intermediate diameter ratios (70% to 80%), there is compressive yielding of the xylem at the base of the smaller branch at its outer edge, before the bifurcation splits at its apex (Fig.1a). In the Type II failure mode, which occurs most often when the two branches are nearer to the same diameter (diameter ratios > 80%), there is no compressive yielding and the bifurcation fails by a sudden splitting of tissues at its apex (Fig.1b). In much lower diameter ratio bifurcations (< 70%), yielding of the branch under compression then tearing of its tissues under tension near the bifurcation becomes a common mode of failure (Fig. 1c), which is termed a 'branch failure'.

Figure 1: Type I and Type II and branch failure modes of tree bifurcations under tension across the bifurcation. In Type I failure mode, the xylem yields initially under compressive forces on the outer edge of the bifurcation before the bifurcation splits at its apex under tension. In Type II failure mode the initial failure is under tension at the bifurcation apex. In branch failures, the initial failure is compressive buckling of the xylem on the underside of the branch before the top of the branch is torn apart under tension.

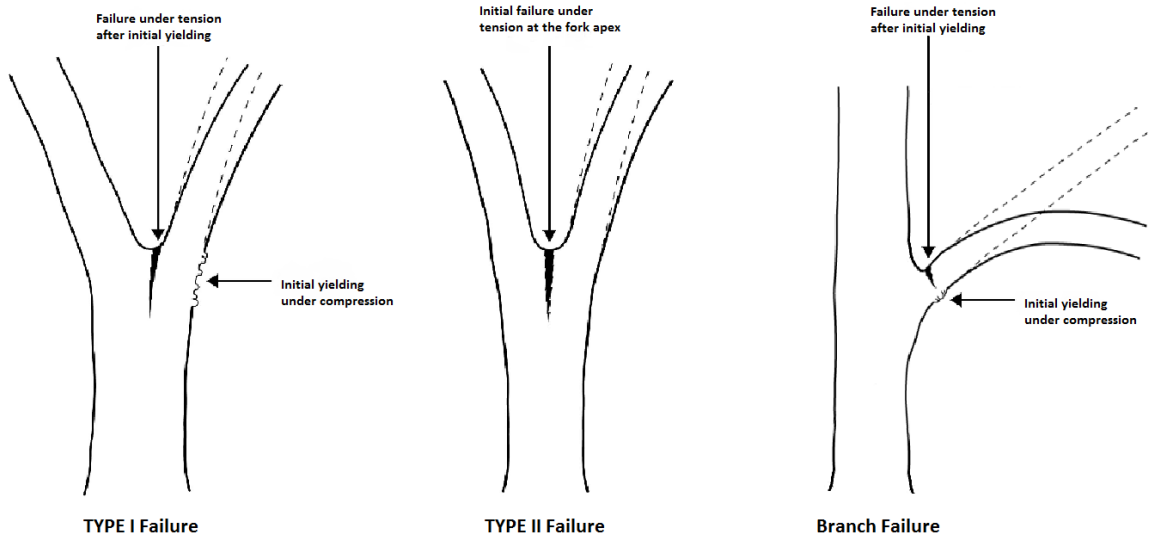

The strength of a normally-formed hazel bifurcation can be considered to be provided by three components: the resistance of wood at the centre of the join to tension, the resistance of wood at either side of the centre of the join to tension and the bending resistance of the wood at the side of the smaller branch as it joins the other branch. The tensile strength of a bifurcation in a tree is increased by it having a zone of interlocking wood grain in the centre of the join (Slater and Ennos, 2013; Slater *et al*, 2014).

Once bark is included into a bifurcation it is inherently weakened as the centrally-placed interlocking wood grain is absent at the apex (Slater *et al*, 2014). Smiley (2003) found that young tree bifurcations with bark inclusions in *Acer rubrum* L. were 20% weaker when pulled apart than those without bark inclusions. A bifurcation with included bark may not remain a significant defect as it matures; it may develop in ways that affect both the relative size of the bark inclusion and the shape of the bifurcation overall. A bifurcation may grow to completely occlude the bark inclusion (Fig. 2: embedded), so it is invisible from the outside; it may form additional xylem around and above the bark inclusion without fully occluding it (Fig. 2: cup-shaped bifurcation); or the bark inclusion may persist and remain at

roughly the same proportion of the width of the join with every annual increment of growth (Fig. 2: wide-mouthed bark inclusion).

Figure 2: Potential development pathways for a bark inclusion, showing the morphology of the xylem perpendicular to the plane of the bifurcation, leading to the formation of embedded bark, a cup-shaped bifurcation, or a wide-mouthed bark inclusion.

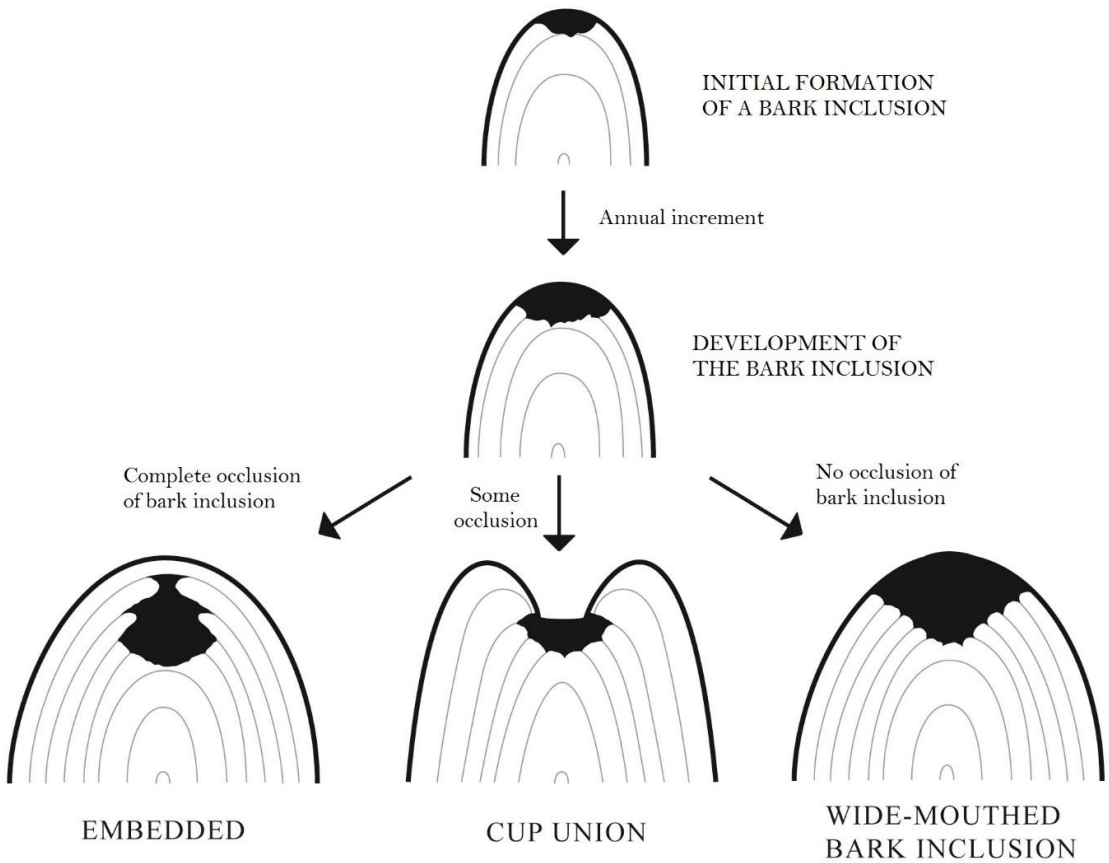

In arboricultural guidance on this commonly-occurring structural flaw, Lonsdale (2000) suggests that the length of the bark inclusion that is visible along the branch bark ridge below the apex of a bifurcation may be linked to the likelihood of its failure. Helliwell (2004) has also suggested that there may be an influence on the strength of a bifurcation with included bark from the degree of constriction of the parent stem's diameter just below the apex of the bifurcation where the bark

inclusion starts. Kane *et al.* (2008) found that the percentage area of the fractured attachment covered by a bark inclusion in red maple (*Acer rubrum*), sawtooth oak (*Quercus acutissima*) and callery pear (*Pyrus calleryana*) did not reliably predict the strength of the bifurcation, but that overall the strength of bark-included bifurcations was lower than normally-formed bifurcations.

Despite these general observations by experienced arboriculturists, there is currently no means of quantifying the heightened risk of failure of bifurcations with included bark in trees from observing their external morphology or the position and size of the bark inclusion present. In this study, therefore, we investigated the strength of bifurcations in relation to the presence or absence of bark inclusions, and, if present, the position, shape and size of bark inclusions found. We sought to find a simple rule by which the relative weakness of a bifurcation with included bark could be predicted.

We chose to model this mechanical behaviour in one species, *Corylus avellana* L., as similar research on this species has been carried out by Pfisterer (2003) which allows for a comparison in findings, and the wood grain orientation and mechanical contributions of different components of such bifurcations in this species have recently been uncovered (Slater and Ennos, 2013). We have favoured this species as an experimental subject as it provides a sustainable source of bifurcations and working with coppice grown material of one species limits the effects of other factors (e.g. age differences, differences in levels of exposure) that could affect bifurcation strength. Having a more comprehensive picture of the biomechanics of bifurcations in one woody species which has been well-researched in respect of its anatomy and mechanical behaviour justifies this single species choice in this study.

Testing the strength of young tree bifurcations may provide useful insight for tree assessors where they inspect larger-growing tree species with bark included junctions, although this approach will likely have its limitations in terms of the scale of the tree bifurcations tested. An important limitation to consider is that young tree bifurcations will consist mostly of juvenile wood, whose mechanical behaviour is different from wood in mature tree boughs. It would therefore be errant to assume that findings from testing young bifurcations could be directly applied to the much larger bifurcations of mature trees.

Materials and Methods

Between November 2010 and January 2012, 241 junctions of hazel were harvested from hazel coppice situated at Prestwich Country Park, Manchester. All the junctions harvested had two emergent branches, making each one a 'bifurcation'. Collecting from only one site was necessary to limit the number of factors affecting bark inclusion formation and bifurcation strength: for example, if one collected from more exposed and more sheltered locations the strength of the individual bifurcations within the sample would vary much more widely. Collection of the samples was randomised throughout the coppice, avoiding obtaining more than two bifurcations from any one tree and not taking any bifurcations from trees growing along the edges of the coppice. This resulted in 96 samples being collected from the same tree as one other sample, and 145 samples each being the only one collected from a particular tree.

Samples were cut to retain approximately 100 mm of the parent stem and 215 mm of each branch arising from the bifurcation. Samples were wrapped separately in

plastic bags and put in cold storage at 2-3°C to reduce sap loss before testing. The hazel bifurcations had an average parent stem diameter of 33.2 mm (range 17.01 mm to 58.69 mm) and an age range of between three to eight years old

Rupture tests were carried out to measure the breaking stress of each bifurcation collected. A 6 mm hole was drilled in both arising branches of each bifurcation, approximately 200 mm from the apex of and perpendicular to the plane of the bifurcation. Each of these specimens was then attached via these drill holes to the crosshead and base of an Instron® 4301 Universal Testing Machine (UTM) mounted with a 1 kN load cell, and then subjected to a rupture test, with the crosshead moving upwards at 30 mm min^{-1}. An interfacing computer recorded the displacement (in millimetres) and peak load (in Newtons) at a data rate of ten measurement points per second.

The failure mode was observed closely and recorded for each specimen during this test procedure. The Type I failure mode was categorised by the appearance of ripples caused by compression forces on the outer edge of the smaller branch as it joined the bifurcation, prior to the splitting of the bifurcation apex. Specimens recorded as undergoing Type II failure mode exhibited no compressive yielding in the exterior tissues prior to the bifurcation splitting at its apex. Branch failures were categorised as all those failures that occurred in the arising branch and that did not split the bifurcation apart (Fig. 1).

The following dimensions of each sample were then measured using a metal rule and digital callipers: the diameter proximal to the bifurcation of the parent stem (*PS*), at the base of the branch bark ridge; the diameter of the larger and smaller arising branches in-line with and perpendicular to the plane of the bifurcation (*A1*,

A2, *B1* and *B2*); and the distances between the drill holes (*a*) and between each drill hole and the bifurcation apex (*b* and *c*) (Fig. 3). Together with the peak force and displacement readings from the Instron® UTM, these parameters were used to calculate the maximum bending moment and bending stress for each sample tested.

Figure 3: Measurements taken of the sample bifurcations with digital callipers and a metal rule: The diameter of the parent stem (PS) and the diameters of both arising branches proximal to the bifurcation in the plane of the bifurcation (A_1 and B_1) and the distances between the drill holes and the bifurcation apex (a, b and c). The diameters of both arising branches were also measured perpendicular to the plane of the bifurcation, giving values A_2 and B_2.

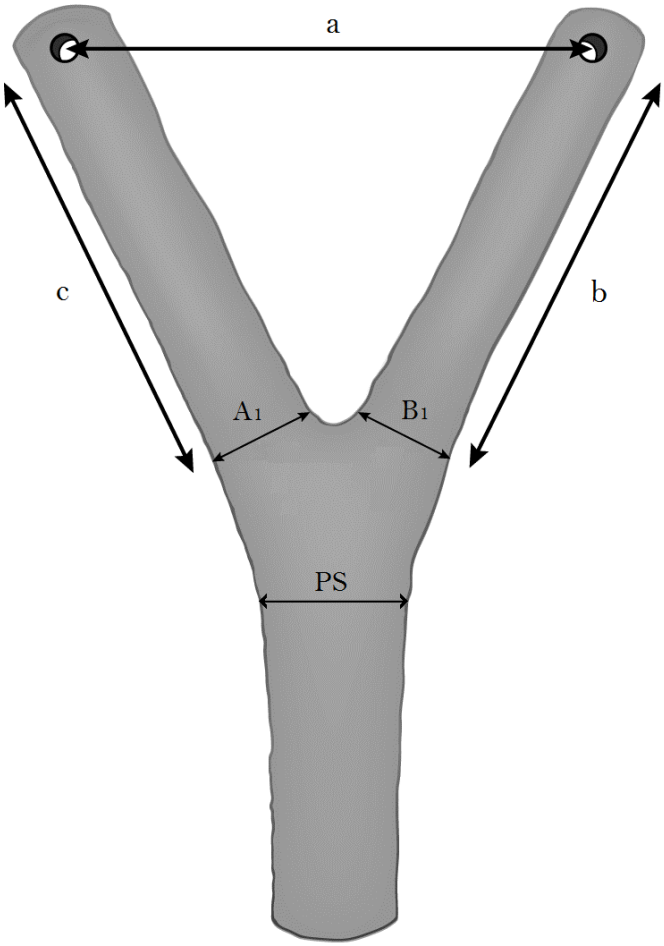

The maximum bending moment, M_{max}, required to break each bifurcation was calculated using the equation

$$M_{\max} = F_{peak}\, b\, Sin\, \alpha \qquad \textit{(Equation 1)}$$

where F_{peak} is the peak force, b is the length between the drill hole in the smaller branch of the specimen to the mid-point of the base of the smaller branch at the apex of the bifurcation and α is the angle at which the force is applied relative to the bearing of length b (Fig. 3).

The angle α was calculated in degrees using the formula

$$\alpha = Cos^{-1} \frac{(a+ext)^2 + b^2 - c^2}{2(a+ext)b} \qquad \text{(Equation 2)}$$

where $(a + ext)$ is the distance between the two drilled holes in the two members of the bifurcation at the point when peak force was recorded, b is the distance between the drill hole in the smaller branch and the apex of the branch bark ridge and c is the distance between the drill hole in the larger branch and the apex of the branch bark ridge (Fig. 3).

To normalise the bending strength of the bifurcations in relation to their different sizes, the maximum bending moment was divided by the section modulus of the elliptical cross-section of the smaller branch of the bifurcation at its point of attachment. The result is maximum bending stress, σ_{fmax}, for each bifurcation and was calculated using the following equation:

$$\sigma_{f\max} = \frac{32 M_{\max}}{\pi B_1^2 B_2} \qquad \text{(Equation 3)}$$

where B_1 and B_2 are two diameters of the smaller branch at its base, taken respectively in line with and perpendicular to the plane of the bifurcation (Gere and Timoshenko, 1996).

After the rupture testing, a three point bending test was carried out on the smaller of the branches arising from the bifurcation to determine the bending stress it could withstand before yielding. All the branches were carefully checked that they had not been damaged during the rupture testing prior to this three point bending, to ensure this testing gave reliable results. This second test was done to allow a comparison between branch strength and bifurcation strength, based on estimations of yield stresses at the base of the smaller branches during the rupture tests (Equation 3) and at the middle of the smaller branches during the three point bending tests (Equation 4). Limitations of the load-cell available meant that branches above the diameter of 23 mm could not be bent to their yield point, limiting the sample size for this second test to 83 branches.

In this three point bending test, the smaller branch was placed upon steel supports set 295 mm apart and a semi-circular plastic probe of 30 mm diameter, attached to a 1 kN load cell in the crosshead of the testing machine, was lowered until it was in contact with the middle of the supported branch. The span length available for these tests was necessarily limited to 295 mm because of the location of two side columns on the Instron® UTM. The testing machine's crosshead was then driven downwards at a rate of 35 mm min^{-1}, bending the branch until it failed, while an interfacing computer recorded a graph of force versus displacement. This loading rate has been successfully used in previous experiments of this nature (van Casteren and Ennos, 2010; Slater and Ennos, 2013).

This test was used to calculate the maximum bending stress, σ_{bmax}, acting upon the branch before it yielded using the equation

$$\sigma_{bmax} = \frac{8\, P_{max}\, L_{span}}{\pi\, D_{mid}^{2}\, W_{mid}} \qquad \text{(Equation 4)}$$

where P_{max} was the maximum load and L_{span} was the distance between the supports, D_{mid} and W_{mid} were the diameters of the branch in-line with and perpendicular to the load respectively, measured where the plastic probe was in contact with the branch during the test (Gere and Timoshenko, 1996).

The completion of the rupture tests and three-point bending tests allowed a comparison to be made between the maximum bending stresses of the bifurcations tested with the maximum bending stresses of the smaller branches that arose from these bifurcations.

Morphological Measurements

Measurements of Included Bark

For all the bifurcations where bark inclusions were exposed during the rupture testing (n = 104), the fracture surfaces were then excised and digitally scanned using an HP Scanjet 2400® (Manufacturer: Hewlett Packard, Palo Alto, California). These samples were then categorised as either embedded bark inclusions (n = 17), cup unions (n = 57) or wide-mouthed bark included bifurcations (n = 30) (Fig. 2). The image analysis software ImageJ® (Abramoff, Magalhaes and Ram, 2004) was then used to measure the area of bark relative to that of the fracture surface (Fig.4a). The same technique was used to measure the ratio between the width of

the bark inclusion at the apex of the bifurcation and the width of the parent stem at the base of the branch bark ridge, where the pith of the parent stem bifurcates (Fig. 4b). This second measure was chosen as we suspected that as the highest tensile stresses act at the bifurcation apex when the two branches are pulled apart, so the failure would occur more easily when a higher proportion of included bark was present in this location.

Figure 4: Measurements of the fracture surfaces of bark-included bifurcations carried out in Image J. **A:** Proportion of the area of the fracture surface containing included bark. **B:** Relative width of the bark inclusion at the apex of the bifurcation, when compared with the width of the parent stem, at the point where the pith bifurcates.

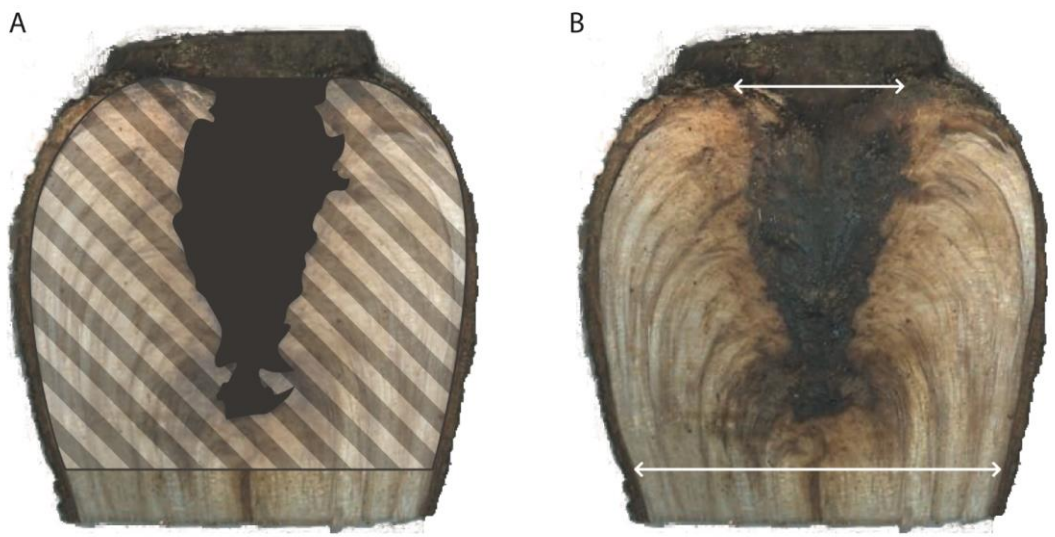

The bifurcations with included bark that was exposed at the apex (n = 87) were also categorised as to whether they had formed a cup-like bifurcation (where two areas of xylem were found at the apex of the bifurcation, formed either side and above the bark inclusion), or whether there was included bark situated at the apex of the

bifurcation (Fig. 5a and b). Again, this comparison was chosen to try to assess if there was a difference in the strength of these two types of bark included bifurcation because of the difference as to which material (wood or bark) was situated at the apex.

Figure 5: Simple visual categorisation of bifurcations with included bark into two types so that their strength could be compared: **A**: cup-shaped bifurcation with wood at its apex or **B**: bifurcation with included bark at its apex.

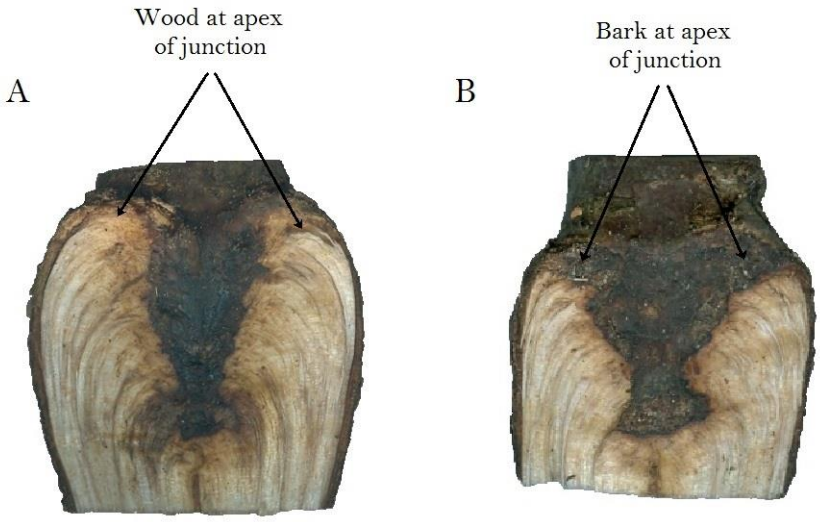

Statistical analysis

A Chi-Squared test was used to determine if there was a significant difference in failure mode between bifurcations with included bark and normally-formed bifurcations.

To analyse the relationship between different failure modes observed and the diameter ratio of the samples tested, a GLM ANOVA was carried out with one covariate (the diameter of the parent stem) and with the random factor of the tree number from which each sample was collected. A post-hoc Tukey test with 95%

confidence interval was used to confirm statistical differences between groups of samples exhibiting different failure modes.

To analyse the relationship between the displacement of the sample prior to failing and the failure modes exhibited by the samples, a GLM ANOVA with post-hoc Tukey test was used, with the diameter of the parent stem as covariate. A subsequent one-way ANOVA was used to determine if bark-included bifurcations exhibiting a Type II failure mode had significantly shorter displacements before failure than normally-formed bifurcations.

A one-way ANOVA, alongside a post-hoc Tukey test with 95% confidence interval, was used to find differences in sample strength between normally-formed bifurcations, bifurcations with included bark and smaller arising branches.

The relationship between the maximum breaking stress, σ_{fmax}, and the shape of the bark inclusions in the bifurcations with included bark exposed at their apex (n = 87) was investigated using stepwise regression analysis. Samples with embedded bark (n = 17) were excluded from this analysis as they did not have a width of bark at the apex of the bifurcation. These stepwise regressions were performed to identify the best models for predicting bifurcation strength from the parameters that were measured for each sample (the diameter ratio, the parent stem diameter, the proportional area of included bark on the fracture surface and the ratio of the bark width at the bifurcation apex with the parent stem diameter) could predict bifurcation strength better.

A GLM ANOVA, alongside a post-hoc Tukey test with 95% confidence interval, were used to confirm differences between groups of categorised bark-included

bifurcations and normally-formed bifurcations, again with the diameter of the parent stem as a covariate and with the number of the tree collected from as a random variable.

Residuals from these ANOVAs and regressions were tested for normality using the Anderson-Darling test to ensure the data were suitable for analysis by parametric statistical tests.

All statistical tests were carried out in Minitab® 16 statistical software.

Results

The range of diameter ratios found in the sample was from 53% to 100%, with the mean ratio being 81.41% ± 0.7 SE. There was no significant difference in the average branch diameter ratio between bifurcations with or without included bark; diameter ratios of the two branches were 80.8% ± 1.0 SE for the normally-formed bifurcations and 82.1% ± 1.1 SE for bifurcations with included bark. Neither did the two types of bifurcation show a significant difference in the relative incidences of the three failure modes ($X^2_2 = 4.224$; $p = 0.121$) (Table 1); in both, Type II failure modes were commonest and branch failures least common.

Table 1: Instances of different failure modes experienced (n) and associated average diameter ratios (μ) of control and bark included forks subjected to tensile testing

Specimen type	**Branch failure**	**Type I failure**	**Type II failure**
Control	n = 9 μ = 76%	n = 53 μ = 74%	n = 73 μ = 86%

Bark included junctions	n = 6 μ = 66%	n = 29 μ = 76%	n = 71 μ = 86%

A subsequent GLM ANOVA showed that there were significant differences between these three modes of failure due to difference in diameter ratio ($F_{2, 236} = 6.28$; $p = 0.004$); the parent stem diameter was not a significant co-variant ($F_{1, 236} = 3.82$; $p = 0.057$) and the random factor of the tree number was not significant ($F_{192, 236} = 0.78$; $p = 0.866$). The higher the diameter ratio, the more common were Type II failure modes and the less common were Type I failure modes and branch failures. A post-hoc Tukey test (CI = 95%) confirmed that this difference was significant between the Type II failure mode and the other two failure modes observed (Fig. 6).

Figure 6: Failure modes in relation to the diameter ratio between the two branches of each bifurcation that underwent a rupture test. Letters above the bars mark

heterogeneity in the sample groups, as determined by a GLM ANOVA and post-hoc Tukey test with 95% confidence interval.

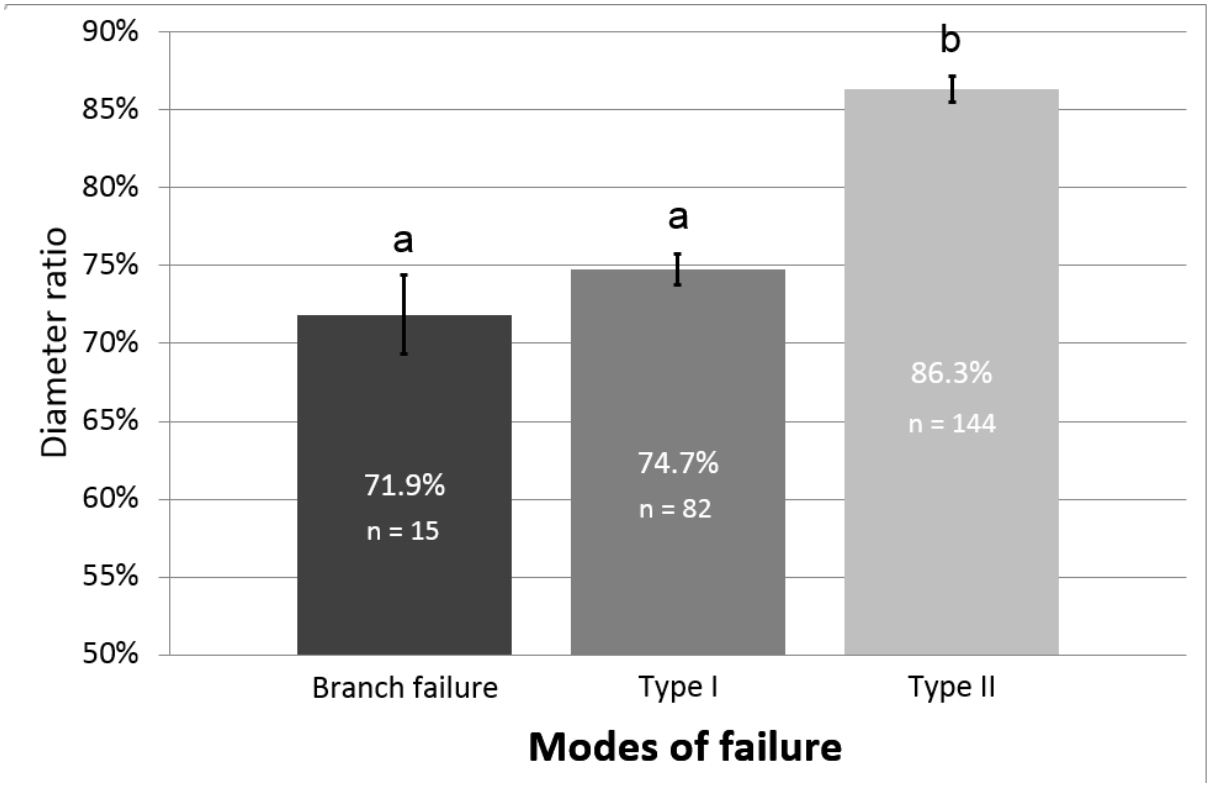

Mean displacements of samples prior to yielding were 135.26 mm ± 15.18 SE for branch failures, 83.04 mm ± 5.08 SE for Type I failures and 37.17 mm ± 1.55 SE for Type II failures. A GLM ANOVA identified that there was a statistical difference between these three groups in terms of the extent of their displacement prior to yielding ($F_{2, 236} = 89.59$; $p < 0.001$); the parent stem diameter was not a significant co-variant ($F_{1, 236} = 0.08$; $p = 0.774$). A post-hoc Tukey test (CI = 95%) confirmed that this difference was significant between all three failure modes, identifying that branch failures occurred after the greatest displacement and Type II failure modes after the least displacement. The mean displacement for Type II failures of normally-formed bifurcations was 43.32 mm ± 2.29 SE, whereas the mean displacement for Type II failures of bark-included bifurcations was 30.85 mm ± 1.8. Analysis of these specimens exhibiting Type II failure mode using a one-way ANOVA and post-hoc Tukey test (CI = 95%) found that bark-included bifurcations

that exhibited the Type II failure mode had a smaller displacement before peak force was reached than the normally-formed bifurcations ($F_{1,\ 142} = 18.18$; $p < 0.001$).

Figure 7 shows typical examples of the force/displacement graphs of the rupture tests on the hazel bifurcations that suffered the Type I and the Type II failure modes in normally-formed bifurcations, a typical branch failure and the typical failure of a bifurcation with included bark at its apex. It can be seen that a long phase of plastic yielding occurs in both branch failure and in Type I failure mode of bifurcations without included bark (Fig.7), with large subsequent deflections before the maximum force is reached. In contrast, in Type II failure mode, there is a sharp drop in force due to fracture after only a very short phase of yielding, while in the bifurcation with included bark, even though it is undergoing Type II failure mode, there is apparent plastic yield at a lower force and a more gradual reduction in force after failure.

Figure 7: Typical force/displacement graphs for specimen types

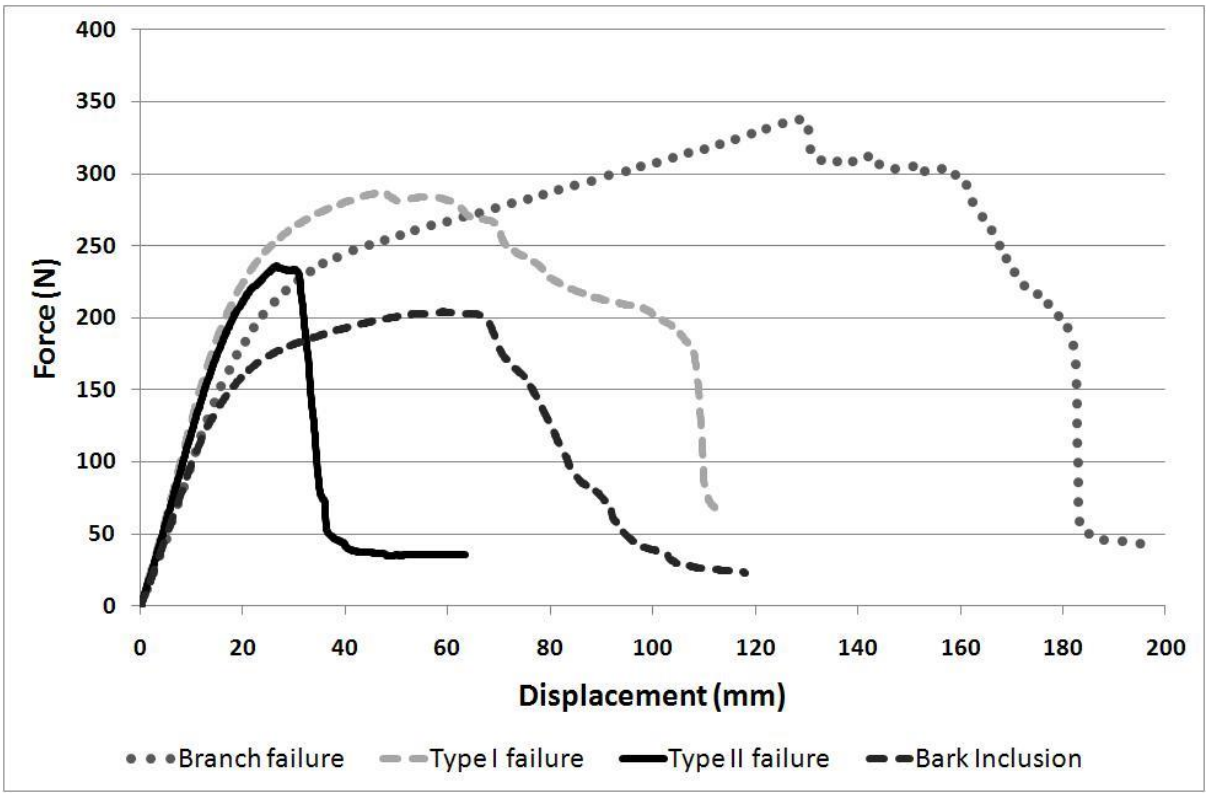

The maximum stresses for the branches subjected to three point bending tests (σ_{bmax}), and for the normally-formed bifurcations and those with included bark subjected to rupture tests (σ_{fmax}) are shown in Figure 8. Bark included bifurcations were on average 24.3% weaker than ones without included bark, which were in turn 13.6% weaker than the smaller branch. A one way ANOVA identified a significant difference in bending stresses for these three groups ($F_{2, 320} = 112.25$; $p < 0.001$), the residuals were found to be normally distributed ($AD_{323} = 0.402$; $p = 0.358$) and a post-hoc Tukey test (CI = 95%) confirmed that each group's mean yield stress was significantly different from the other groups.

Figure 8: Mean yield stress of branches, normally-formed bifurcations and bifurcations with included bark. Columns labelled with different letters are

significantly different, as determined by a one-way ANOVA and post-hoc Tukey test (CI: 95%).

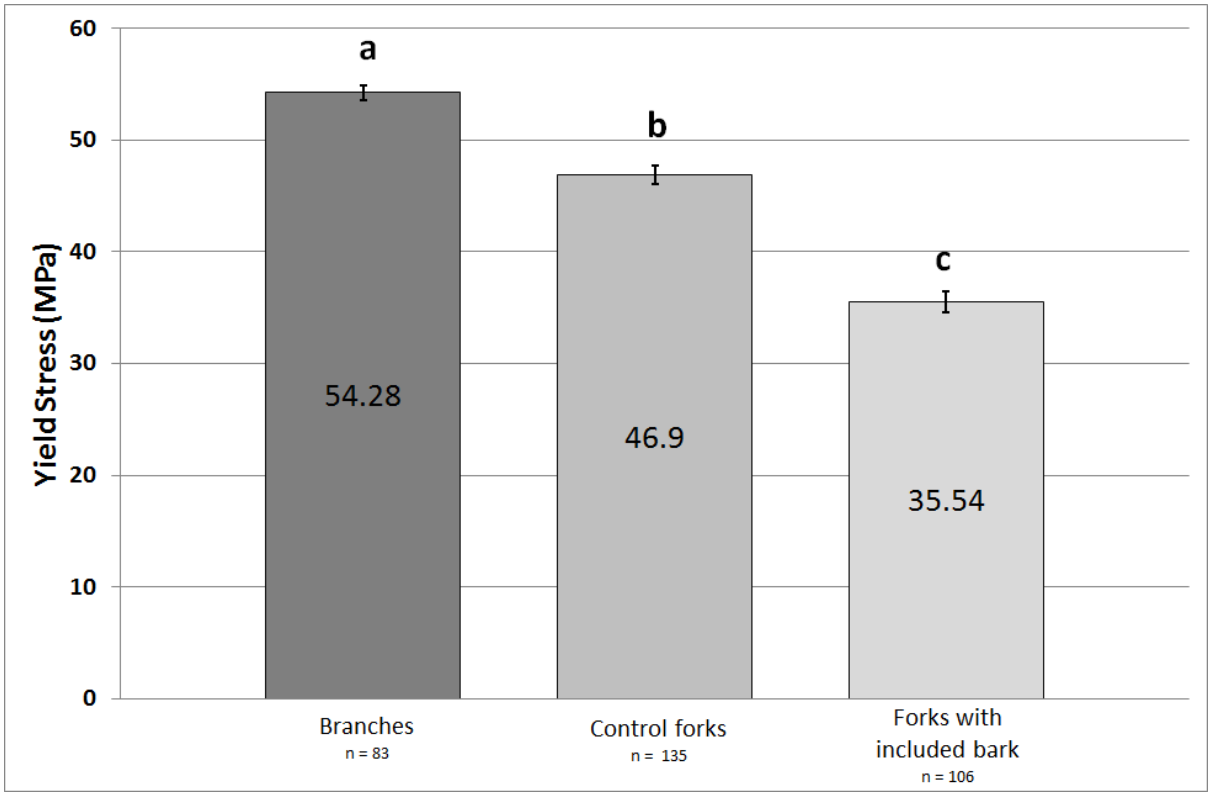

Effects of the Extent and Location of Included Bark

The first regression model that identified a significant relationship used a combination of the diameter ratio (t_{84} = 4.42; p < 0.001) and the area of the bark inclusion (t_{84} = 2.38; p = 0.02). The overall model fit was R^2 = 0.21 and the best fit line was given by the equation:

$$\text{Yield stress (MPa)} = 69.9 - 35.2\,r - 24.6\,a \qquad \text{(Equation 5)}$$

where r is the diameter ratio of the two branches of the bifurcation (as a percentage with a maximum of 100%) and a is the area of bark as a percentage of the entire fracture surface (maximum value 100%) from the point of the bifurcation of the pith to the apex. The diameter ratio predicted 15.8% of the variability in the

sample, the area of the bark inclusion only a further 5.3% using this model (equation 5). When the factor of parent stem diameter was added to this regression model, it did not significantly improve the prediction of breaking strength (t_{83} = 1.04; p = 0.302).

The second regression model found to be significant using the stepwise regression approach identified a stronger relationship using a combination of the diameter ratio (t_{84} = 4.57; p < 0.001) and width of bark inclusion (t_{84} = 3.0; p = 0.004). The overall model fit was R^2 = 0.247 and the best fit line was given by the equation:

$$\text{Yield stress (MPa)} = 68.5 - 35.8\, r - 9.27\, w \qquad \text{(Equation 6)}$$

where w is the proportional width of the bark inclusion at the apex of the bifurcation when compared with the width of the parent stem (as a percentage, no maximum limit). The diameter ratio predicted 16.6% of the variability in the sample, the width of the bark inclusion a further 8.1% using this model (equation 6). When the factor of parent stem diameter was added to this second regression model, again it did not significantly improve the prediction of breaking strength (t_{83} = 0.67; p = 0.502).

The mean maximum breaking stress (σ_{fmax}) of normally-formed bifurcations (n = 135) was 46.9 MPa (± 0.8 SE), the mean maximum breaking stress for bifurcations with embedded bark (n = 17) was 44.7 (± 1.79 SE), whereas the mean breaking stress for cup-shaped bark-included bifurcations (n = 57) was 37.02 (± 1.11 SE) MPa, and for those with bark at their apex (n = 30), the mean was 27.22 (± 1.23 SE) MPa. A GLM ANOVA with the parent stem diameter as a covariate ($F_{2, 236}$ = 49.4; p < 0.0001) and tree number as a random variable showed that there were significant

differences between these four groups, and a post-hoc Tukey test (CI = 95%) showed that both the cup-shaped bark-included bifurcations and the wide-mouthed bark inclusions had significantly different mean breaking stresses from each other and from the normally-formed bifurcations and those with embedded bark (Fig. 9). Parent stem diameter was not a significant covariate that affected bifurcation strength ($F_{2, 236} < 0.01$; $p = 0.989$), nor was tree number a significant variable.

Figure 9: Mean yield stress of normally-formed bifurcations, bifurcations with embedded bark, cup-shaped bifurcations and bifurcations with wide-mouthed bark inclusions at their apices. Columns labelled with different letters are significantly different, as determined by a GLM ANOVA and post-hoc Tukey test (CI: 95%).

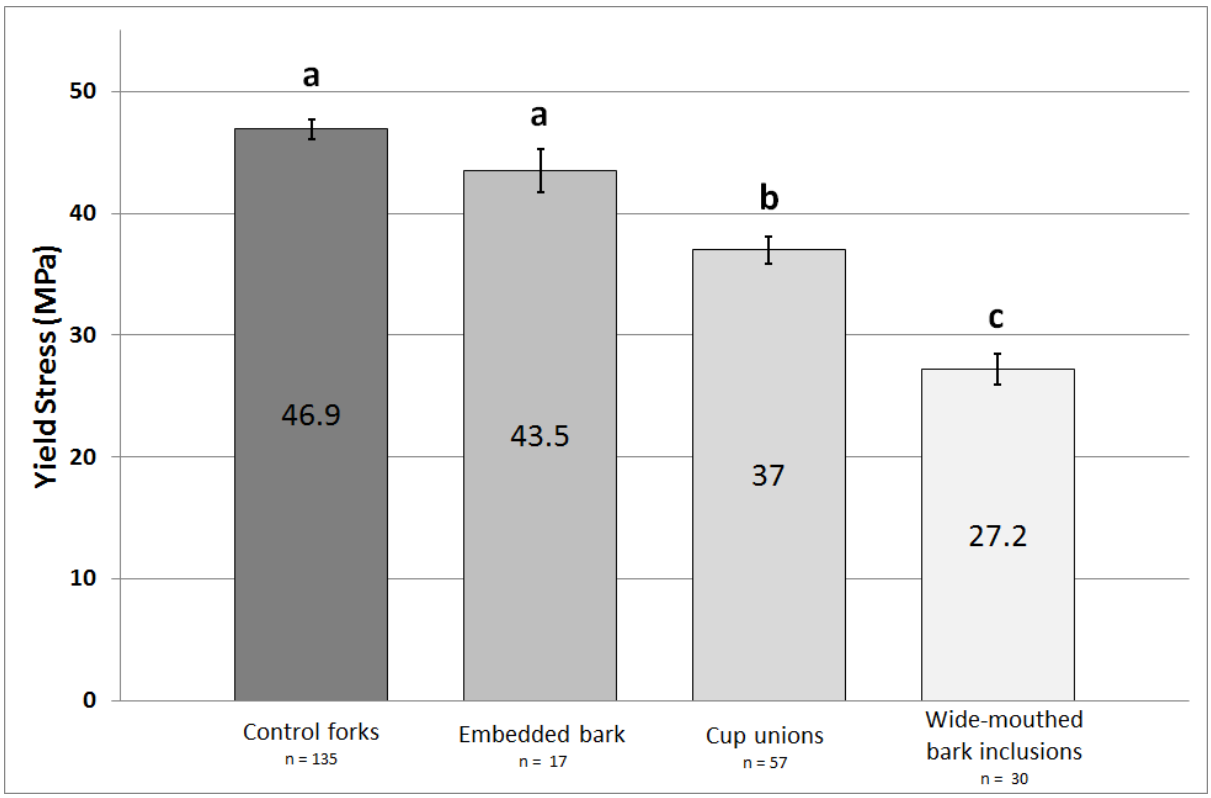

Discussion

The results from this study show that there are gradations in the strength of bark-included bifurcations in young hazel plants that relate to the scale and position of the bark inclusion and their level of occlusion within the wood formed at these bifurcations. These factors were found to be independent of the size of the specimens, where this was assessed by recording the diameter of the parent stems just below the bifurcation (which varied from 17.01 mm to 58.69 mm). However, there was considerable variability in the sample that remains unexplained from the simple regression models used here, which explained only a quarter of the variation in strength found in the sample bifurcations.

Firstly, it is clear that the diameter ratio of the branches has a greater influence on the strength of hazel bifurcations in static rupture tests than does the extent of the bark inclusions. In both normally-formed and bark-included bifurcations, those consisting of two branches of similar diameter are weaker and are more likely to fail by Type II failure mode than those with a lower diameter ratio. Secondly, the presence of a bark-inclusion does weaken hazel bifurcations to a similar degree as was found by Smiley (2003) in *Acer rubrum* and that the extent of weakening increases with the width of the bark inclusion at the apex of the bifurcation. However, there was still a large degree of variability in this sample, so accurate predictions about the strength of a bifurcation cannot be made simply from examination of this aspect of its external morphology. The variability may be mainly due to differences in the reorientation of wood grain at the apices of the bifurcations, as this provides a key strengthening component (Slater *et al.*, 2014).

Diameter ratio can have a significant effect on the failure mode of bifurcations in trees (Gilman, 2003; Kane *et al.*, 2008). In the case of these hazel samples, boundaries for different failure modes can be set by their diameter ratios. For the samples tested, a diameter ratio higher than 80% most frequently resulted in Type II failure mode, a lower ratio than that led to most of the Type I failure modes until the ratio of 72% was reached, where branch failures started occurring and only branch failures occurred at a ratio of 55% and below. It should be noted that the bifurcations of hazel were selected to have a relatively high diameter ratio between their two branches so as to successfully investigate bifurcation failures, so consequently the incidence of branch failures was low in the test specimens.

Type I failures of bifurcations showed a greater displacement prior to yielding than did Type II failures (Fig. 7): this is explained by the initial stage of Type I failure, where wood at the outer edge of the bifurcation is yielding under compression until sufficient stress is concentrated at the bifurcation apex to split the xylem tissues situated there. Branch failures, using this form of rupture test, displayed a much extended displacement during testing, as there was a great deal of yielding under compression on the underside of the branch prior to any break of fibres under tension on the upper side (van Casteren and Ennos, 2010). The force/displacement graphs often showed a different behaviour where a bark inclusion was present, with a longer phase of plastic deformation as the bifurcation 'crept apart' rather than exhibiting a distinct breaking point – however, for those exhibiting Type II failure mode, the peak force was reached with less displacement in bark-included bifurcations than with normally-formed bifurcations. The absence of interlocking wood grain at the apex of these bark-included bifurcations is an obvious reason for this difference in mechanical behaviour (Slater *et al.*, 2014). These results corroborate the findings of Pfisterer (2003), who also found

differences in behaviour in hazel bifurcations with and without bark inclusions, but who did not differentiate between Type I and Type II failure modes.

The higher tensile strength of bifurcations with a higher diameter difference in their branches is ascribed by Gilman (2003) to the level of occlusion of the smaller branch into the other stem. However, it may be more appropriate to think about this relationship in terms of the loading caused by the different bending behaviours of the branches in the wind (Fig. 10).

Figure 10: Suggested contrast in bending behaviour between a low diameter ratio bifurcation and a high diameter ratio bifurcation

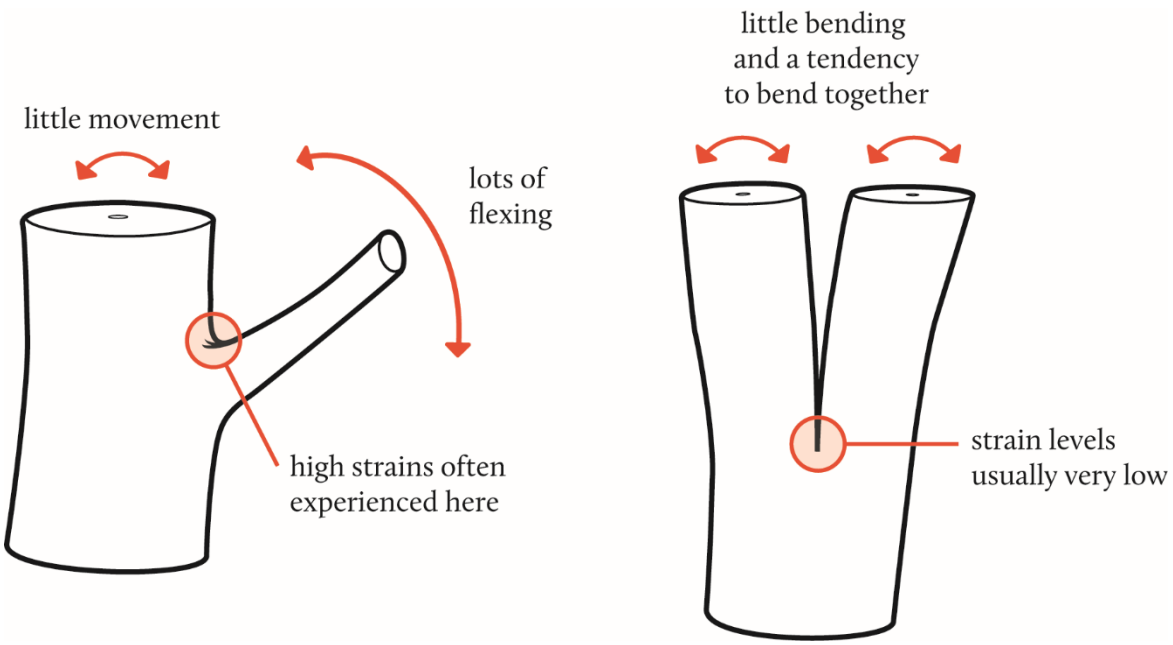

From preliminary research work we have undertaken using accelerometers attached just above bifurcations in hazel, the frequency and extent of oscillations separating apart a smaller diameter branch and a larger diameter branch where their bases are conjoined at a bifurcation will both be greater than when two branches of equal diameter are bent in a wind of the same force. As a consequence of experiencing higher strain levels more regularly at its apex through this different

bending behaviour, lower diameter ratio bifurcations are likely to develop a higher level of modification of their tissues to adequately resist those forces (Metzger, 1893; Jaffe and Forbes, 1993; Telewski, 1995). In contrast, the bifurcation with included bark is a structure where little to no strain is regularly experienced at its apex, so no substantial resources are committed by the tree to reinforcing it.

Bifurcations with bark inclusions were on average only three-quarters the strength of the normally-formed specimens, but there was a wide range of peak stress values, with some bark-included samples experiencing branch failure rather than splitting at the bifurcation itself and other bark-included bifurcations having less than 40% of the bending strength of the smaller branch.

A simple analysis of the strength of the bifurcations with included bark and their morphology provided two useful insights. Firstly, it can be concluded that small areas of embedded bark do not give rise to a significant difference in bifurcation strength. Secondly, cup-shaped bifurcations in hazel were significantly stronger than those that had bark at their apex. The conclusion from these findings is that the main reason why the strength of bifurcations with included bark was found to be so variable in the tested specimens was that the areas of included bark in the samples were at different stages of occlusion at the bifurcation apex: a higher level of occlusion of the bark inclusion resulted in an increase in the bifurcation's strength. Thus the cup-shaped bifurcations tested in this study represented different stages of repair of the structural flaw that was caused by the initial inclusion of bark into those junctions.

From this experiment, we can provide an interpretation of the mechanical performance of bifurcations with included bark in trees, from our testing of these

hazel specimens; however, it is very important to recognise the limitation of this study, in that young bifurcations of only one species that contained solely juvenile wood were tested, and the mechanical behaviour of mature bifurcations in different woody species may well vary from what we found in our samples.

Wide-angled bifurcations which are U-shaped at their apex and without bark inclusions and bifurcations with embedded bark should both be considered adequate structures as there should be interlocking wood grain present at the bifurcation apex. Where a significant width of included bark is found at the apex of the bifurcation, this indicates a significantly weaker bifurcation and a tree assessor should evaluate the proportional width of this bark in relation to the overall width of the join perpendicular to the plane of the bifurcation. They should also take into account the extent of adaptive growth at each side of the bifurcation, the extent of occlusion of the bark inclusion by the formation of a cup-shaped bifurcation and, most critically, whether the level of wind exposure of the bifurcation has been heightened by recent site changes or pruning works. The rapid formation of additional xylem that lies at either side of a bifurcation (often indicated by a change in bark texture) may be an indication of instability of that bifurcation (Mattheck and Breloer, 1994).

Features to survey for in bark-included bifurcations, based on this study using hazel specimens, are identified in Figure 11.

Figure 11: Weaker and stronger forms of bifurcations with included bark. **A:** A wide-mouthed bark-inclusion positioned at the apex of the bifurcation, with acutely pointed reaction growth forming below the inclusion. **B:** A cup-shaped bifurcation

with two rounded areas of abnormal growth at the apex of the bifurcation that act to resist bending stresses

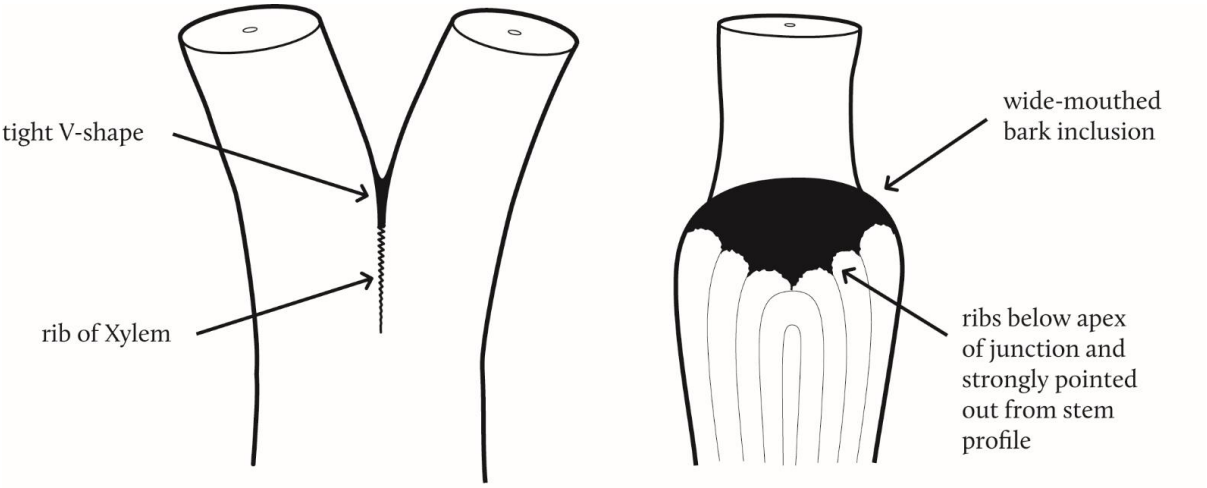

A: junction that is 33% weaker than control fork

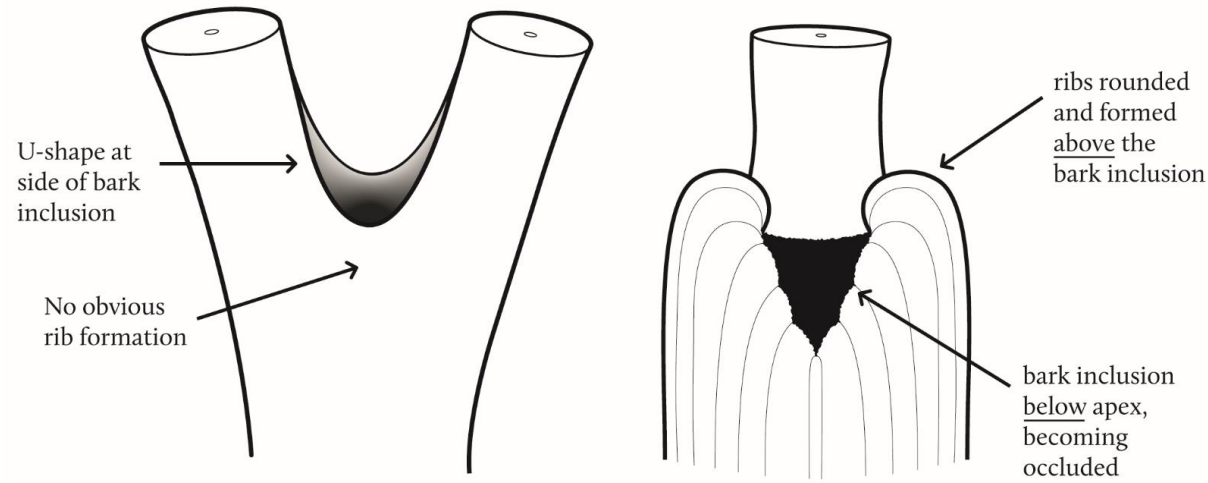

B: cup union that has similar strength to control fork

It would seem that a bark-included bifurcation's notoriety as a defect in trees comes from the risk of this structure being exposed to a wind event or other loading event that causes the two arising branches to oscillate or move apart in a way that has not frequently occurred during the bifurcation's prior development. This problem can be accentuated by arboricultural practices like crown thinning, felling

of adjacent trees or the transplanting of trees into new locations, where these practices would lead to abrupt changes in the level of exposure to which the bifurcation is not sufficiently adapted (Wood, 1995).

Studies of the strength of bifurcations with included bark in trees should be taken further. As in this study we tested juvenile wood in only one species, a similar study using mature bifurcations in a range of species would assist in determining their mechanical behaviour. In addition, a better understanding of the forces affecting the modulus of rupture of these bifurcations may come from using finite element analysis to assess stress concentration levels at the apices of such bifurcations. Further study should also determine how frequently and under what particular wind conditions such damaging oscillations occur to bifurcations with included bark. It would also be informative to investigate the movement behaviour of normally-formed bifurcations during dynamic wind loading and to determine to what extent these bifurcations develop their morphology and wood properties in relation to the dynamic forces that act upon them.

Acknowledgements

This research work was sponsored by Myerscough College, Lancashire and supported by staff at the University of Manchester, England.

For the provision of the hazel specimens used in this experiment, the authors' thanks are given to Mike Carswell.

Assistance in the production of figures was kindly given by Mike Heys of Myerscough College.

References

Abramoff, M. D., Magalhaes, P. J., Ram, S. J. 2004. Image Processing with ImageJ; *Biophotonics International* **11** (7), pp. 36-42

Gere, J. M. and Timoshenko S. P. 1996. *The Mechanics of Materials*. 4th edition. Boston: PWS Publishing Co.

Gilman, E. 2003. Branch-to-stem diameter ratio affects strength of attachment; *Journal of Arboriculture* **29** (5) pp. 291-294

Gilman, E. 2011. *An illustrated guide to pruning*; 3rd edition; Cengage Learning

Harris, R. W., Clark, J. R. and Matheny, N. P. 2004. *Arboriculture: Integrated management of landscape trees, shrubs and vines*; p. 38, 4th edition; Prentice-Hall

Helliwell, R. 2004. A discussion of the failure of weak forks. *Arboricultural Journal*, 27**,** 245-249.

Jaffe, M. J. and Forbes, S. 1993. Thigmomorphogenesis: the effect of mechanical perturbation on plants; *Plant Growth Regulation* **12** pp. 313-324

Kane, B., Farrell, R., Zedaker, S. M., Loferski, J. R. and Smith, D. W. 2008. Failure mode and prediction of the strength of branch attachments; *Arboriculture and Urban Forestry* **34** (5) pp. 308-316

Lonsdale, D. 1999. *Principles of Tree Hazard Assessment and Management*; 1st edition; The Stationery Office

Lonsdale, D. 2000. *Hazards from trees: A general guide;* Forestry Commission Practical Guide series; Forestry Commission

Matheny, N. P. and Clark, J. R. 1994. *Evaluation of Hazard Trees in Urban Areas*; 2nd edition; Illinois, USA: International Society of Arboriculture

Mattheck, C. and Breloer, H. 1994. *The body language of trees: A handbook for failure analysis*; The Stationery Office

Metzger, K. 1893 Der wind als massgebender factor für das waschstum der bäume; *Mündener Forstliche Hefte* 3 pp. 35-86

Pfisterer, J. A. 2003. Towards a better understanding of tree failure: Investigations into bending stresses of branch junctions and reiterates of European filbert (*Corylus avellana* L.) as a model organism. *In: Second International Symposium on Plant Health in Urban Horticulture*, August 27-29, 2003 Berlin.

Shigo, A. L. 1989. *Tree pruning: A worldwide photo guide;* pp. 78-83. Durham, New Hampshire: Shigo and Trees, Associates

Slater, D. and Ennos, A. R. 2013. Determining the mechanical properties of hazel forks by testing their component parts; *Trees: Structure and Function* **27** (6) 1515-1524

Slater, D., Bradley, R. S., Withers, P. J. and Ennos, A. R. 2014. The anatomy and grain pattern in forks of hazel (*Corylus avellana* L.) and other tree species; *Trees: Structure and Function* **28** (5), 1437-1448

Smiley, E. T. 2003 Does included bark reduce the strength of co-dominant stems? *Journal of Arboriculture* **29** (2) pp. 104-106

Telewski, F. W. 1995. Wind-induced physiological and developmental responses in trees; pp. 237-263; In: *Wind and Trees*, Coutts M. P. and Grace J. eds.; Cambridge University Press

van Casteren, A., Ennos, A. R. 2010. Transverse stresses and modes of failure in tree branches and other beams; *Proceedings of the Royal Society B: Biological Sciences* **277** (1685) pp. 1253-1258

Wood, C. J. 1995. Understanding wind forces on trees; pp. 133-163; In: *Wind and Trees*, Coutts M. P. and Grace J. eds.; Cambridge University Press